The Journal of Chemical Physics

Energetic preference and topological constraint effects on the formation of DNA twisted toroidal bundles

Cite as: J. Chem. Phys. **158**, 114904 (2023); https://doi.org/10.1063/5.0134710
Submitted: 13 November 2022 • Accepted: 27 February 2023 • Accepted Manuscript Online: 28 February 2023 • Published Online: 16 March 2023

Nhung T. T. Nguyen, Anh T. Ngo and Trinh X. Hoang

The Journal of Chemical Physics ARTICLE scitation.org/journal/jcp

Energetic preference and topological constraint effects on the formation of DNA twisted toroidal bundles

Cite as: J. Chem. Phys. 158, 114904 (2023); doi: 10.1063/5.0134710
Submitted: 13 November 2022 • Accepted: 27 February 2023 •
Published Online: 16 March 2023

Nhung T. T. Nguyen,[1] Anh T. Ngo,[2] and Trinh X. Hoang[1,3,a)]

AFFILIATIONS

[1] Institute of Physics, Vietnam Academy of Science and Technology, 10 Dao Tan, Ba Dinh, Hanoi 11108, Vietnam
[2] Chemical Engineering Department, University of Illinois at Chicago, Chicago, Illinois 60608, USA
[3] Graduate University of Science and Technology, Vietnam Academy of Science and Technology, 18 Hoang Quoc Viet, Cau Giay, Hanoi 11307, Vietnam

[a)] **Author to whom correspondence should be addressed:** txhoang@iop.vast.vn

ABSTRACT

DNA toroids are compact torus-shaped bundles formed by one or multiple DNA molecules being condensed from the solution due to various condensing agents. It has been shown that the DNA toroidal bundles are twisted. However, the global conformations of DNA inside these bundles are still not well understood. In this study, we investigate this issue by solving different models for the toroidal bundles and performing replica-exchange molecular dynamics (REMD) simulations for self-attractive stiff polymers of various chain lengths. We find that a moderate degree of twisting is energetically favorable for toroidal bundles, yielding optimal configurations of lower energies than for other bundles corresponding to spool-like and constant radius of curvature arrangements. The REMD simulations show that the ground states of the stiff polymers are twisted toroidal bundles with the average twist degrees close to those predicted by the theoretical model. Constant-temperature simulations show that twisted toroidal bundles can be formed through successive processes of nucleation, growth, quick tightening, and slow tightening of the toroid, with the two last processes facilitating the polymer threading through the toroid's hole. A relatively long chain of 512 beads has an increased dynamical difficulty to access the twisted bundle states due to the polymer's topological constraint. Interestingly, we also observed significantly twisted toroidal bundles with a sharp U-shaped region in the polymer conformation. It is suggested that this U-shaped region makes the formation of twisted bundles easier by effectively reducing the polymer length. This effect can be equivalent to having multiple chains in the toroid.

I. INTRODUCTION

In DNA condensation, extended DNA chains collapse into highly compact structures, which contain only one or a small number of molecules.[1,2] The condensation can occur spontaneously *in vitro* upon adding a small amount of multivalent cations, such as spermidine^{3+}, to a buffered solution of low ionic strength.[3] It can also be observed by using polymeric osmolytes, such as small peptides or PEG, as the condensing agents.[4] The packing of DNA inside a condensate is highly ordered and is akin to a nematic liquid crystalline state.[5] The most commonly observed morphologies of DNA condensates are toroid and rod-like.[6] The sizes of these structures depend on the solution condition and range from few ten to few hundred nanometers.[7] Under a certain method of preparation, larger condensates with spheroid and V-shaped morphologies can be observed.[8] Surprisingly, the size of DNA condensates does not depend the contour length of the DNA molecules involved in the condensation.[9]

The phenomenon of DNA condensation has been considered theoretically from the perspective of the collapse of semiflexible polymers into compact structures, often in the form of toroidal and/or rod-like globules. Different aspects of this polymer collapse have been studied in order to deduce the detailed geometry of the condensates and the resulting phase diagram[10–16] and their dependence on the forms of the elastic potential,[17,18] and the DNA–DNA interaction potential,[19] as well as to elucidate the nature of the collapse transition[20,21] and kinetic pathways.[22–25]

There has been much focus on the structural organization of DNA in toroidal condensates. In a DNA toroid, the DNA winds around the toroid main axis, making a tight circular bundle. The lateral packing of the filaments inside the toroid is predominantly hexagonal,[26] but the structure also contains non-hexagonal parts.[27] Using cryo-electron microscopy, Leforestier and Livolant have shown that the DNA toroidal bundle inside the bacteriophage capsid is twisted with a number of twist walls, the portions of the toroid in which the hexagonal lattice is rotated, separating non-rotated hexagonal domains.[28] Earlier indirect indications of a twisted state come from experiments[29,30] and simulations,[31] which show that the path of DNA inside the toroids does not follow the spool-like packaging, and also from the strong knotting of DNA in phage capsids.[32] Based on experimental observations, Hud *et al.* have proposed a constant radius of curvature model[30] for the organization of DNA in the toroids, which is akin to a twisted bundle. A more elaborate model of a twisted bundle has been analyzed by Kulić *et al.*, showing that twisting can spontaneously relax the bending energy of the toroidal bundle.[33] However, the formation of such twisted bundles by a single or multiple DNA chains in a toroid is still not well understood, which is part of a more general problem of packing of twisted filament bundles.[34]

The present study is aimed at better understanding the twisted state of toroidal bundles formed by semiflexible polymers. We focus on whether the twisted bundles are competitive in energy among several kinds of bundle organization, such as in the constant radius of curvature model, and whether such a twisted state is the ground state of a stiff polymer chain with self-attraction. To get insights into these issues, we employ a combined approach of using both theoretical models and coarse-grained molecular dynamics simulations, allowing a comparison between the two methods. We consider two slightly different models for the twisted toroidal bundles, one with a uniform and the other with a variable degree of twisting, to compare with other models corresponding to spool-like and constant radius of curvature arrangements. The simulations of the stiff polymers are carried out both with the replica-exchange molecular dynamics (REMD) method[35] for finding low energy conformations and with constant temperature molecular dynamics for studying the toroid formation process.

We will show that a moderate twisting significantly increases the stability of a toroidal bundle, while the topological constraint of a long polymer may affect its ability to form a twisted bundle. Interestingly, the results obtained from the simulations are in good agreement with the theoretical models.

II. MODELS AND METHODS

A. Twisted bundle models

In a twisted toroidal bundle within a toroid of mean radius R and thickness radius Δ as shown in Fig. 1(a), the DNA conformation has the parameterized form[33]

$$\mathbf{r}(\rho,\theta,\phi) = \begin{pmatrix} (R-\rho\,\cos\,\theta)\cos\,\phi \\ (R-\rho\,\cos\,\theta)\sin\,\phi \\ \rho\,\sin\,\theta \end{pmatrix}, \tag{1}$$

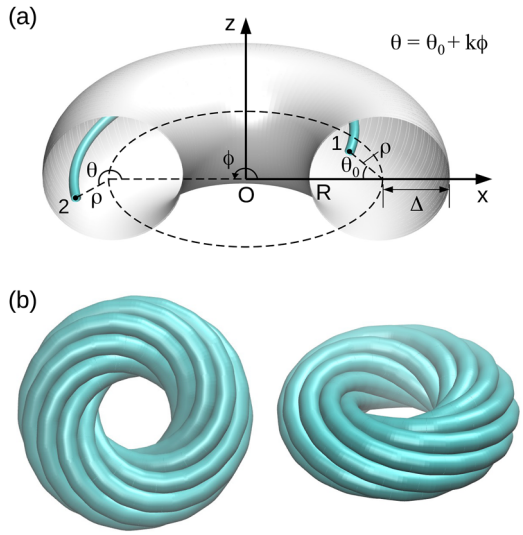

FIG. 1. (a) Sketch of the coordinates of a toroidal bundle. The toroid's tubular axis (dashed circle) is set to be centered at the origin O of the Cartesian coordinates on the xy plane. A DNA filament is shown from point 1 to point 2 inside the torus (only half of which is shown). The filament trace is determined by the radial distance ρ from the tubular axis, the rotation angle ϕ around the main axis z, and the rotation angle θ within the tubular cross section. R and Δ are the toroid's mean radius and thickness radius, respectively. For the twisted toroidal bundle, $\theta = \theta_0 + k\phi$, where θ_0 is a θ's value at $\phi = 0$ and k is the twist number. (b) Illustration of a twisted toroidal layer formed by a single chain with $k = 0.73$ at two different viewing angles.

with $\theta = \theta_0 + k\phi$ and the column on the right having the x, y, and z components of the vector $\mathbf{r}$. In this parameterization, $\mathbf{r}$ is the position of the DNA molecular axis, $\rho \in (0, \Delta)$ is the radial distance from the toroid's tubular axis, ϕ and θ are the rotation angles around the main and tubular axes, respectively, and k is a parameter that sets the degree of twisting. k defines how much the change in θ is faster than the change in ϕ along the filament and is hereby called the twist number. Such a bundle is organized into disconnected toroidal layers of filaments at constant ρ as shown in Fig. 1(b).

Denote $\mathbf{r}' = d\mathbf{r}/d\phi$. It can be shown that

$$|\mathbf{r}'| = \sqrt{(k\rho)^2 + (R-\rho\,\cos\,\theta)^2}, \tag{2}$$

which gives the differential of the arc length s of a filament, $ds = |\mathbf{r}'|d\phi$. The tangent $\mathbf{t}$ is defined as

$$\mathbf{t} = \frac{d\mathbf{r}}{ds} = \frac{1}{|\mathbf{r}'|}\frac{d\mathbf{r}}{d\phi}. \tag{3}$$

The normal $\mathbf{n}$ and the binormal $\mathbf{b}$ are defined through the Frenet–Serret equations,[36]

$$\frac{d\mathbf{t}}{ds} = c\,\mathbf{n}, \quad \frac{d\mathbf{n}}{ds} = -c\,\mathbf{t} + \tau_s\mathbf{b}, \quad \frac{d\mathbf{b}}{ds} = -\tau_s\mathbf{n}, \tag{4}$$

which also define the curvature c and the torsion τ_s of the DNA axis. From the parameterization in Eq. (1), c can be obtained in a closed form, whereas τ_s is more conveniently calculated numerically. Due to the toroid symmetry, both c and τ_s are functions of ρ and θ only.

Given that d is the lateral distance between neighboring DNA filaments and $\eta = \pi/(2\sqrt{3})$ is the volume fraction of a hexagonal packing, the total length of DNA in the toroid is given by

$$L = \frac{\eta V_{\text{tor}}}{\pi(d/2)^2} = \frac{8\pi\eta\Delta^2 R}{d^2}. \tag{5}$$

One can write the bending energy of the toroidal bundle in the volume integral form

$$U_{\text{tor}} = \frac{\eta}{\pi(d/2)^2}\int_0^{\Delta} d\rho \int_0^{2\pi} \rho\, d\theta \int_0^{2\pi} (R - \rho\,\cos\,\theta)\,\frac{A}{2}c^2\, d\phi, \tag{6}$$

where A is the DNA bending stiffness.[37] Note that this form of bending energy implies a uniform density of DNA inside the toroid, or equivalently, a constant spacing d within the toroid. The latter is an approximation since a recent experiment has shown that this spacing decreases with increasing distance from the toroid center.[38]

We adopt an energy function for the toroid that includes only bending and surface energy terms,

$$E_{\text{tor}} = U_{\text{tor}} + \sigma S_{\text{tor}}, \tag{7}$$

where σ is the surface tension and $S_{\text{tor}} = 4\pi^2\Delta R$ is the toroid's surface area. The present model neglects the twist degree of freedom of the DNA double helix and also assumes that the chain is inextensible. These are reasonable approximations given that the molecule is not under torque nor under tension. Indeed, it can be shown that the twist energy in toroids due to the twist-bend coupling[39] is negligible (see Sec. IV). However, it should be noted that our model also neglects the helical structure of DNA, which may give rise to the twisting of DNA bundles.[28]

Let us call $\alpha = \Delta/R$ the thickness radius to mean radius ratio or, shortly, the thickness ratio. The equilibrium configuration of the toroid is obtained by minimizing the energy with respect to α and k. Hence, E_{tor} plays the role of free energy at a constant temperature. In numerical calculations, we set $d = 2.8$ nm and the DNA bending stiffness $A = 50$ nm $\cdot\, k_BT$, with k_B the Boltzmann constant and T the absolute temperature. Energy is given in units of k_BT.

We consider two models of twisted toroidal bundles. In the first model, namely, the twisted bundle (TB) model, the twist number k is independent of ρ and, thus, is uniform in the whole toroid. This model is identical to the conventional model considered elsewhere.[33] The second model allows k to be varied with ρ and, thus, is hereby named the twisted bundle model with a ρ-dependent twist number (TB-ρ model). In both models, k is optimized by minimizing the toroid energy.

B. Spool-like model

The spool-like (Sp) model[30] is a special case of the TB model with $k = 0$. In the Sp model, the curvature is given by

$$c = \frac{1}{R - \rho\,\cos\,\theta}, \tag{8}$$

and the bending energy in Eq. (6) can be exactly calculated giving

$$U_{\text{tor}}^{\text{Sp}} = \frac{8\pi\eta A}{d^2}\,(R - \sqrt{R^2 - \Delta^2}). \tag{9}$$

C. Constant radius of curvature model

The constant radius of curvature (CC) model[30] sets a uniform curvature of DNA within the toroid with the radius of curvature equal to the toroidal mean radius R. Such a model is formed by loops being deposited spirally around the toroid circular axis (see Ref. 30). The bending energy in this model is equal to

$$U_{\text{tor}}^{\text{CC}} = \frac{A}{2}\frac{L}{R^2}. \tag{10}$$

D. Stiff polymer model with self-attraction

We also consider a stiff polymer model for studying the toroid formation by molecular dynamics simulations. The model considers a chain of N beads with the potential energy given by

$$E_p = \sum_{i=1}^{N-1} K(r_{i,i+1} - b)^2 + \sum_{i=1}^{N-2} \kappa_b(1 - \mathbf{u}_i \cdot \mathbf{u}_{i+1}) + \sum_{i<j+2} \epsilon\left[e^{-2(r_{ij}-d_0)/\lambda} - 2e^{-(r_{ij}-d_0)/\lambda}\right], \tag{11}$$

where the first term contains harmonic potentials for the chain connectivity with the equilibrium bond length b and spring constant K, the second term is a worm-like chain or Kratky–Porod's type of bending energy[37,40] with κ_b the stiffness per bead, and the last term corresponds to non-local interactions given by the Morse potential[15] with the potential depth ϵ, the equilibrium length d_0, and the decay length λ. $r_{i,i+1} = |\mathbf{r}_{i+1} - \mathbf{r}_i|$ is the distance between beads i and $i+1$. $\mathbf{u}_i$ is a normalized vector given by

$$\mathbf{u}_i = \frac{\mathbf{r}_{i+1} - \mathbf{r}_i}{r_{i,i+1}}. \tag{12}$$

r_{ij} is the distance between bead i and bead j. All the beads are assumed to have the same mass m. For the simulations, we consider b, m, and ϵ as the length, the mass, and the energy units, respectively. The parameters chosen for the model are $K = 100\epsilon/b^2$, $\kappa_b = 22\epsilon$, $d_0 = 1.4b$, and $\lambda = 0.24b$. Given that the DNA thickness is about 2 nm, which is equivalent to b, the chosen values d_0 and λ are close to those of the intermolecular potential in multivalent cation condensed DNA measured by osmotic stress.[41]

To analyze the twist degree of a toroidal structure of the polymer obtained by the simulations, we first fit the polymer conformation to a perfect torus. The torus center is the center of mass of the polymer. The main axis of the torus is determined by diagonalizing the inertia tensor of the polymer conformation. The mean radius R is obtained by minimizing the root mean square distance of all the beads of the polymer from the tubular axis. A local tangent vector at the bead i of the polymer is defined as

$$\mathbf{t}_i = \frac{\mathbf{r}_{i+1} - \mathbf{r}_{i-1}}{|\mathbf{r}_{i+1} - \mathbf{r}_{i-1}|}. \tag{13}$$

The local twist number of the bead i at the distance ρ from the tubular axis and with the toroidal rotation angle θ is calculated as

$$k_i = \frac{(R - \rho\,\cos\,\theta)\,t_\phi}{\rho\, t_\theta}, \tag{14}$$

where $t_\phi = \mathbf{t}_i \cdot \mathbf{e}_\phi$ and $t_\theta = \mathbf{t}_i \cdot \mathbf{e}_\theta$ are the ϕ- and θ-components of the tangent vector, respectively, with $\mathbf{e}_\phi$ and $\mathbf{e}_\theta$ the unit vectors along the corresponding rotational directions.

E. Replica-exchange molecular dynamics (REMD)

The replica-exchange molecular dynamics (REMD) method[35] is implemented to find the ground state of the stiff polymers. In this method, one simulates multiple copies (or replicas) of a system at various constant temperatures and regularly attempts swap moves that exchange the replica conformations at neighboring temperatures with associated velocity rescaling. The exchange probabilities are determined such that the detailed balance condition is satisfied at each temperature.[42] This parallel tempering technique has been widely used in molecular simulations and is very efficient for obtaining equilibrium characteristics as well as the ground state of a system. In our REMD simulations, the constant temperature runs for the replicas were carried out by using a molecular dynamics method based on the Langevin equation.[43] For a given polymer, 16–30 replicas were simulated at a range of temperatures that span from a high temperature corresponding to the swollen phase of the polymer to a low temperature near zero. The swap moves were attempted every 10τ, where $\tau = (mb^2/\epsilon)^{1/2}$ is the simulation's time unit. The lengths of the simulations are of the order of $10^6\tau$ for each replica. For each polymer length, up to 24 independent REMD simulations were carried out. The ground state is considered to be the lowest energy conformation if the same conformation was obtained in several runs.

III. RESULTS

We first studied the characteristics of the four models of toroidal bundles: TB, TB-ρ, Sp, and CC, described in Sec. II. For a given DNA length L and a surface tension σ, the toroid energy is minimized with respect to the thickness ratio $\alpha = \Delta/R$ with $\alpha \in (0, 1)$ in all the models. In the TB and TB-ρ models, the energy is also minimized with respect to the twist number k and $k(\rho)$, respectively. Typical toroids have L from 15 to 30 μm, whereas a giant toroid can reach $L \sim 10^3$ μm. The value of σ can be estimated from the intermolecular potential $\Phi(d)$ for DNA measured by the osmotic stress experiment[41] as $\sigma = -\frac{\Phi(d)}{d}$.[15] Consider an example of $L = 30$ μm and $\sigma = 0.15 k_B T/\text{nm}^2$. The TB model has the energy minimum at the optimal twist number $k^* \approx 0.738$, as shown in Fig. 2. This energy minimum is substantially lower than the lowest energy of the toroid in the Sp and CC models with the energy difference from ~70 to ~150 $k_B T$. The TB-ρ model yields an energy of only ~6 $k_B T$ lower than the TB model and is the one that gives the lowest energy among all the models. The above picture of the energy competition is qualitatively the same for all L and σ, indicating that twisting can substantially stabilize the toroidal bundle.

Due to the system's geometry, the optimal twist number k^* in the TB model is a function of the thickness ratio α alone. As shown in Fig. 3(a), k^* is a non-monotonic but primarily decreasing function of α. The values of k^* are bound between the maximum of about 1.12 obtained at the limit of $\alpha = 0$ and the minimum of about 0.66 at $\alpha \approx 0.89$. Similarly, the optimal twist number $k^*(\rho)$ in the TB-ρ model is a function of ρ/R alone. Figure 3(b) shows that the dependence of $k^*(\rho)$ on ρ/R is non-monotonic with a maximum at

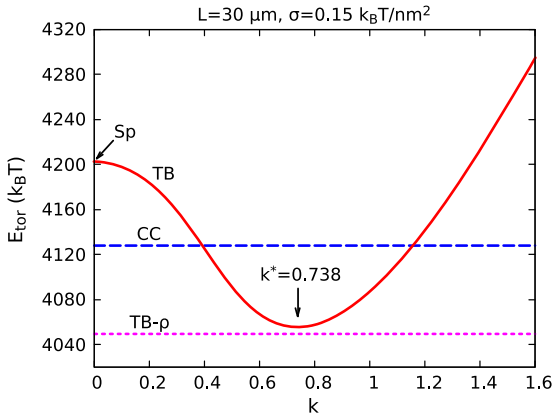

FIG. 2. Dependence of the toroid energy on the twist number k in the twisted bundle model (TB) (solid) for the DNA length $L = 30$ μm and the surface tension $\sigma = 0.15 k_B T/\text{nm}^2$. For each value of k, the energy is minimized with respect to the thickness ratio α. The energy at $k = 0$ corresponds to the spool-like model (Sp). Horizontal lines indicate the toroid energy in the constant radius of curvature model (CC) (dashed) and in the twisted bundle model with a ρ-dependent twist number (TB-ρ) (dotted).

$\rho/R = 0$ and a minimum at $\rho/R \approx 0.81$. The range of $k^*(\rho)$, from 0.55 to 1.12, is slightly different from that of k^*. The ranges of k^* and $k^*(\rho)$ indicate that twisting is moderate in the optimal toroidal bundles.

Figure 4 shows the curvature maps in a tubular cross section of the toroids in the four models considered. These maps, obtained for $\alpha = 0.66$ and suitably at optimal values of k and $k(\rho)$, show that

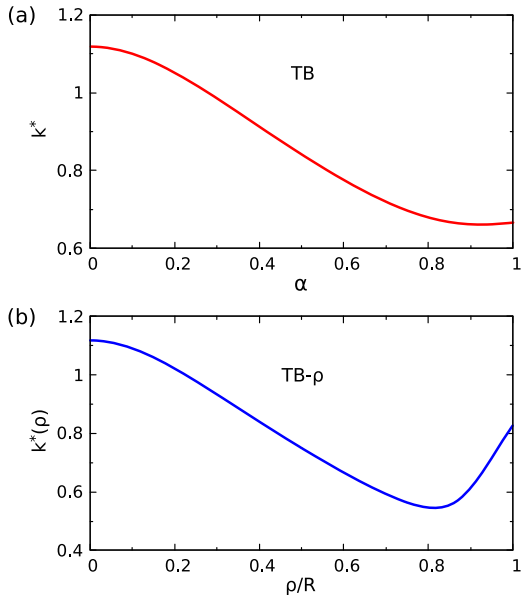

FIG. 3. (a) Dependence of the optimal value of the twist number, k^*, on the toroid's thickness ratio α in the TB model. (b) Dependence of the optimal value of the ρ-dependent twist number, $k^*(\rho)$, on the ratio ρ/R in the TB-ρ model.

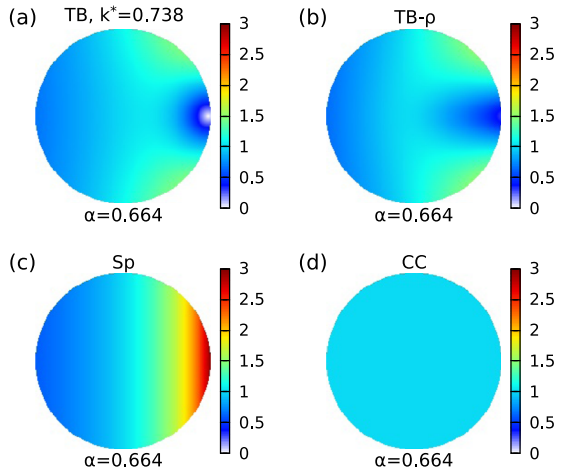

FIG. 4. Curvatures of DNA in modeled toroids with a thickness ratio $\alpha = 0.664$. The curvatures, with values indicated by the color bar in units of R^{-1}, are shown as color maps for a tubular cross section of the toroidal bundles in the TB (a), TB-ρ (b), Sp (c), and CC (d) models. The toroid in the TB model is shown with the optimal twist number $k^* = 0.738$. The right edge of the cross section corresponds to the inner edge of the toroid.

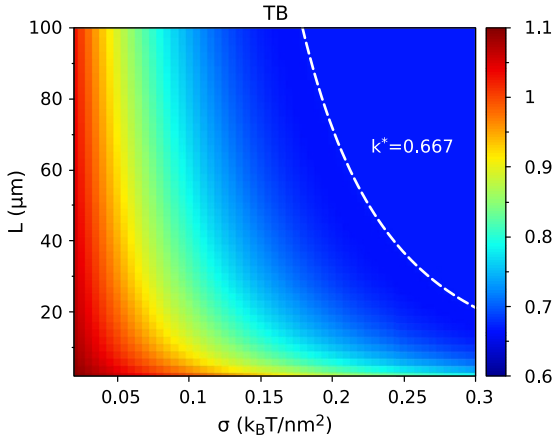

FIG. 5. Dependence of the optimal twist number, k^*, on the DNA length, L, and the surface tension, σ, of toroidal condensates in the twisted bundle model. The values of k^* are shown by a heat map with colors indicated by the associated color bar. The dashed line indicates the boundary of a map region in which k^* is constant ($k^* = 0.667$). In this region, the toroid has no hole ($\alpha = 1$). The boundary has the shape of $L \sim \sigma^{-3}$.

the TB and TB-ρ models have a broad spot of low curvatures near the inner edge of the toroid (the right edges of the cross sections in Fig. 4). At this region of the cross section, the curvatures are the highest in the Sp model. This difference clearly shows the effect of twisting on lowering the curvatures of the bundles. On increasing α, we find that the low curvature spot in the TB and TB-ρ models is slightly shifted away from the inner edge of the toroid (see Fig. S1 for $\alpha = 0.9$), but the qualitative picture is unchanged. No big difference is seen in the curvature maps of the TB and TB-ρ models, indicating that these two models work similarly.

Figure 5 shows the dependence of the optimal twist number, k^*, on the DNA length, L, and the surface tension, σ, as a heat map for the toroidal bundles in the TB model. It can be seen that k^* gradually decreases from the top values to some minimum value on increasing L or σ with the gradient in σ much higher than in L. There is a region in the top right of the σ–L plane where k^* is constant and equal to 0.667. This region corresponds to the toroids with $\alpha = 1$ or the toroids with no holes (see also Fig. S2). The boundary of this region is found to have a shape of $L \sim \sigma^{-3}$ in the σ–L plane, indicating an invariance of α and, hence, k^* by rescaling σ with $L^{1/3}$.

In fact, in all the models considered, the properties of toroidal bundles are invariant with the scaled quantity $(\sigma/A)L^{1/3}$. Figure 6 shows that the thickness ratio α increases with $(\sigma/A)L^{1/3}$ in all the models considered, but the toroids in the TB and TB-ρ models have a higher thickness ratio than in the CC and Sp models for the same $(\sigma/A)L^{1/3}$. The value of α, therefore, reaches 1 faster in the TB and TB-ρ models on increasing L or σ. These two twisted bundle models also yield very similar values of α, as shown in Fig. 6.

Finally, we carried out REMD simulations of stiff polymers with self-attraction to study the toroid formation. We fixed the stiffness per bead of these polymers to be $\kappa_b = 22\epsilon$ and studied various chain lengths of $N = 64$, 128, 256, and 512 beads. For the stiffness and length considered, the simulations show that the polymers form toroids at low temperatures and rods at intermediate temperatures. Figures 7(a)–7(d) show the lowest energy conformations obtained by the simulations for these systems, all of which have a toroidal shape. For $N = 64$, 128, and 256, the conformations shown in Fig. 7 are very likely the ground state of the corresponding system as we have obtained very similar conformations of similar energies in several independent simulations. For $N = 512$, this is less likely due to the large system size and the decreased dynamical accessibility of the lowest energy states [the lowest energy conformation in Fig. 7(d) was obtained only once]. Interestingly, all these ground state and lowest energy structures appear as twisted toroidal bundles with the polymer winding repeatedly from the outer perimeter to the inner hole of

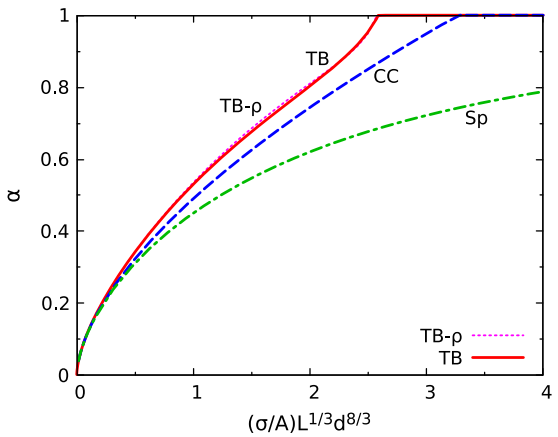

FIG. 6. Dependence of the thickness ratio α on the scaled and dimensionless quantity $(\sigma/A)L^{1/3}d^{8/3}$ for toroidal bundles in the TB (solid), TB-ρ (dotted), CC (dashed), and Sp (dotted) models, as indicated. In all models, the toroid energy is minimized with respect to geometrical parameters.

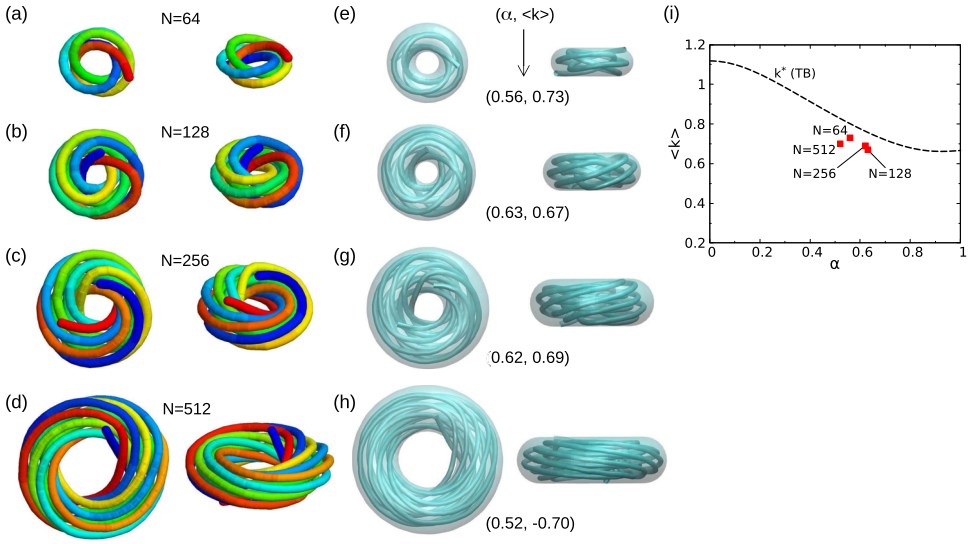

FIG. 7. (a)–(d) Toroid conformations obtained by REMD simulations in the self-attractive stiff-polymer model with $\kappa_b = 22\epsilon$. The conformations shown are the lowest energy conformations for the chain lengths $N = 64$ (a), $N = 128$ (b), $N = 256$ (c), and $N = 512$ (d). Each conformation is shown at two different viewing angles. (e)–(h) Fits of the bundles from left into a perfect torus shown at two different angles. The analyses of the bundles (see Sec. II and Fig. S3) give the estimated values of α and the average twist number, $\langle k \rangle$, for each conformation (numbers in parentheses). (i) Dependence of the average twist number, $\langle k \rangle$, on the thickness ratio α for the toroidal bundles shown in (a)–(d) (squares). The data points are labeled with the corresponding chain lengths. For comparison, the dependence of the optimal twist number, k^*, on α from the TB model is also shown (dashed).

the toroid. They look remarkably similar to the ideal twisted bundle shown in Fig. 1(b).

In order to quantitatively estimate the twist degrees of the lowest energy toroidal bundles, we fitted the polymer conformation to a perfect torus for each system and then calculated the local twist numbers from the local tangent vectors of the polymer (see Sec. II and Fig. S3). The images of the fits are shown in Figs. 7(e)–7(h). Our analysis gives the average twist number $\langle k \rangle \approx 0.73$, 0.67, 0.69, and −0.7, for the $N = 64$, 128, 256, and 512 systems, respectively. The minus sign for the average twist number of the $N = 512$ system stands for an inverse twisting direction of this bundle compared to other bundles. For all the bundles shown in Fig. 7, $\langle k \rangle$ falls within the range of k^* predicted by the TB model. By plotting $\langle k \rangle$ vs α for the lowest energy toroids obtained by simulations, as shown in Fig. 7(i), we find that $\langle k \rangle < k^*$ for all systems considered, but the data points are quite close to the curve of k^* given by the TB model.

Note that we have also obtained many competing toroidal conformations from independent REMD simulations. Some of them are shown in Fig. 8 for the $N = 256$ and $N = 512$ systems. The energies of these conformations are only slightly (less than 2%) higher than the energies of the lowest energy conformations shown in Figs. 7(c) and 7(d). Note that though having low energies, some of these toroidal bundles are only weakly twisted [Figs. 7(c), 7(d), and 7(f)]. Interestingly, some other toroidal bundles are strongly twisted. For example, the conformations shown in Figs. 8(a), 8(b), and 8(e) are even more twisted than the lowest energy conformations in Figs. 7(c) and 7(d). Note that the strongly twisted bundles in Fig. 8 [conformations (a), (b), and (e)] have a sharp U-shaped region in the polymer conformation. It seems that this U-shaped region makes the polymer effectively shorter and, hence, allows easier access to the twisted bundle conformation with some cost in energy.

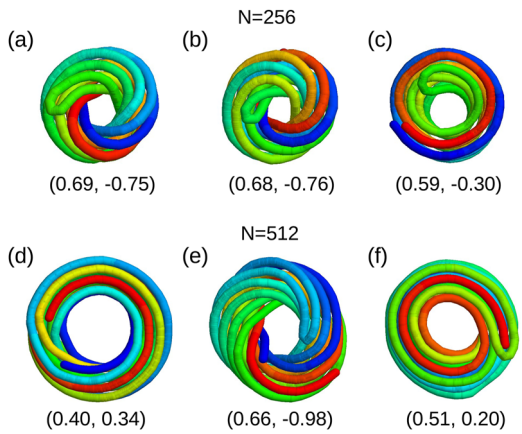

FIG. 8. Some low-energy toroidal conformations obtained in REMD simulations for stiff polymers of lengths $N = 256$ [(a)–(c)] and $N = 512$ [(d)–(f)] with $\kappa_b = 22\epsilon$. The energies of these conformations are higher than but within 2% of the energy of the conformations shown in Figs. 7(c) and 7(d). The two numbers in parentheses under each conformation correspond to the thickness ratio α and the average twist number $\langle k \rangle$, respectively, obtained from the analysis of the bundle. The local twist numbers of the residues in the U-shaped regions are discarded in calculating $\langle k \rangle$.

The REMD simulations carried out above are efficient for energy minimization, but they contain unrealistic conformational changes due to the replica exchange moves. In order to study the toroid formation process with true dynamics, we carried out multiple constant-temperature MD simulations of the stiff polymer of $N = 256$ beads at temperatures T below the collapse transition temperature, which is roughly ~2.7 ϵ/k_B. At $T = 0.5\epsilon/k_B$ and $T = 1\epsilon/k_B$, nearly 40% of the trajectories succeeded in forming a toroid within the simulation time limit of $10^6\tau$ for each temperature. Other trajectories ended up in hairpin-like and rod-like conformations (see Fig. S4), which are known to be metastable states of stiff polymers.[23] At $T = 2\epsilon/k_B$, almost all the trajectories ended up in a toroid within the above time limit. From these simulations, we find that toroids can be formed from extended conformations either through a direct pathway (without intermediates) or through an indirect pathway (with intermediates).

A typical direct pathway can be described by the trajectory shown in Fig. 9, which is obtained at $T = 0.5\epsilon/k_B$. In this trajectory, the extended chain spontaneously forms a loop that nucleates a growth process, resulting in a rapid folding of the chain into a toroid. Once formed, the toroid continues to undergo a quick tightening process and then a slow tightening process, which reduce the toroid diameter and increase its thickness (see conformations in Fig. 9). A sharp drop in energy is associated with both the growth and the quick tightening processes, whereas the slow tightening decreases the energy only slightly and stops when the structure is fully relaxed. Interestingly, the toroid is seen to be twisted early in the tightening processes and in the final structure, indicating that toroidal bundles are prone to twisting with any toroid diameter. Most of the toroids formed with the above-mentioned pathway have no U-shaped region in the final structure. However, depending on the trajectory, the chain may also form a U-shaped region during the growth process (see the example in Fig. S5).

An example of an indirect pathway is shown in Fig. 10 with a trajectory obtained at $T = 1\epsilon/k_B$. In this trajectory, the chain first forms a long hairpin-like conformation (also called one-head racquet conformation[23]), with a length equal to half of the DNA length, as the intermediate state. The hairpin-like conformation then spontaneously forms a loop, which then quickly tightens into a twisted toroidal bundle (the growth process is lacking in this trajectory because the nucleated loop has the full length of the hairpin). The toroid formed via this pathway typically contains the U-shaped region initially belonging to the hairpin. It can be expected that rod-like conformations are the possible intermediates in the toroid formation since they appear as long-lived states in the simulations (Fig. S4). However, the rod to toroid transition can be extremely slow at low temperatures due to high energy barriers. In fact, we did not observe this transition at $T = 0.5\epsilon/k_B$ and $T = 1\epsilon/k_B$ within the given simulation time limit. However, by increasing the temperature, one can easily observe the rod to toroid transition. For example, in a trajectory at $T = 2\epsilon/k_B$ shown in Fig. S6, the chain first forms a rod-like structure that progressively becomes more compact and then transforms into a toroid. It is also found that, on average, the polymer collapse is faster as the temperature is increased within the low-temperature range considered. It can be understood that increasing the temperature makes the stiff polymer more flexible and promotes conformational changes, resulting in shorter times for nucleation loop formation and transitions between metastable states. Note that the change in temperature in our model is equivalent to an inverse change in the interaction strength between DNA segments, which can be modulated by the solvent condition.

The kinetic pathways described above are in agreement with many previous simulation studies of semiflexible polymers[22–25,31] and are supported by the *in vitro* kinetic studies of DNA condensation.[2,6,44,45] A plausible new finding from the present simulations is of the tightening processes, which are subsequent to the

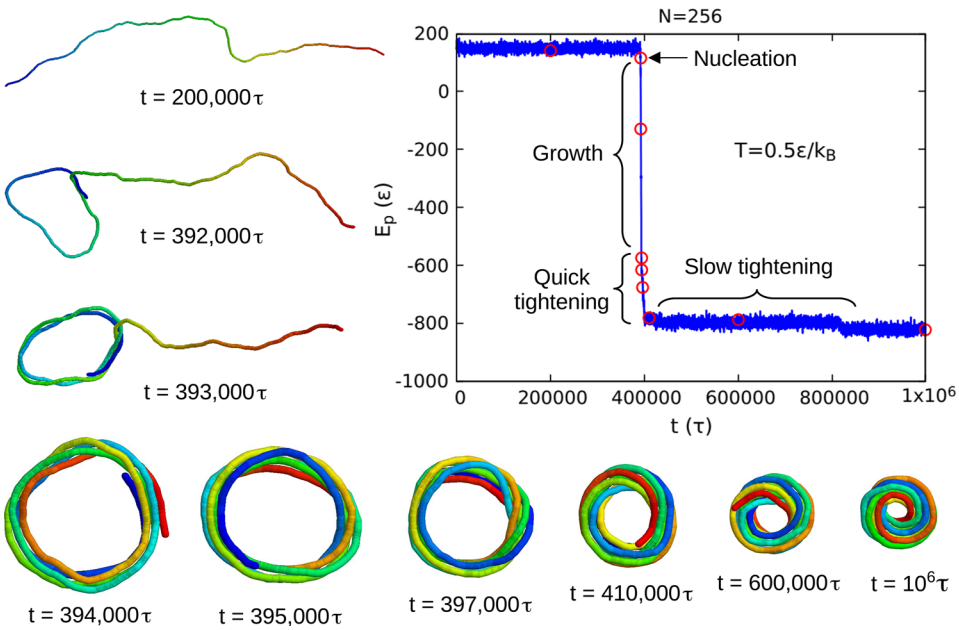

FIG. 9. A simulation trajectory leading to a toroid formation without intermediates. The trajectory was obtained at temperature $T = 0.5\epsilon/k_B$ for a stiff polymer of $N = 256$ beads with the bending stiffness $\kappa_b = 22\epsilon$. The time dependence of the potential energy E_p and a number of conformations drawn from the trajectory at selected points (open circles) are shown. The observed stages of the polymer collapse include nucleation, growth, quick tightening, and slow tightening, as indicated.

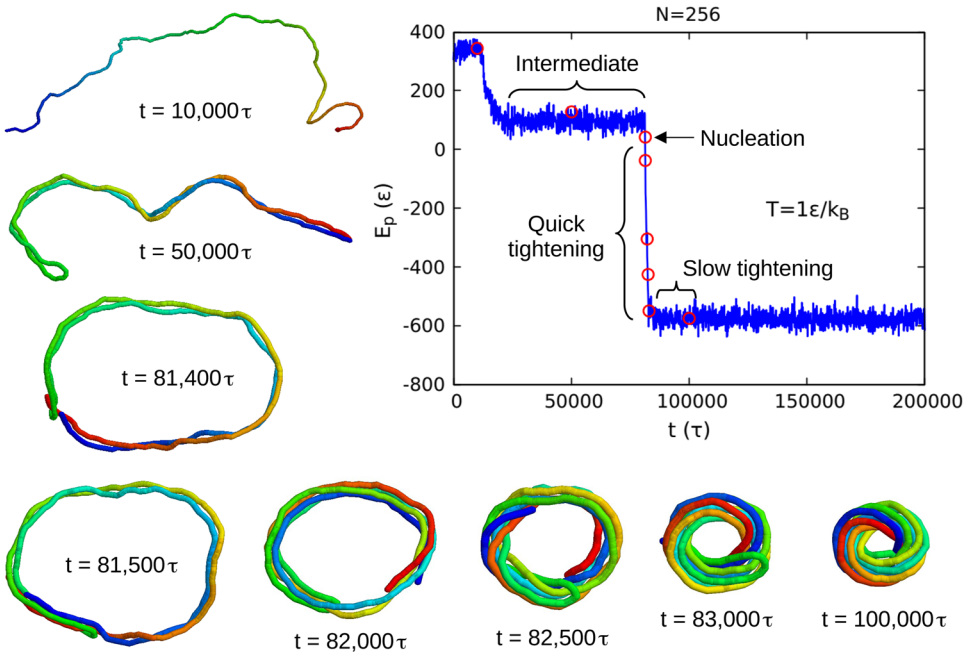

FIG. 10. A simulation trajectory showing the toroid formation through a hairpin-like intermediate. The trajectory was obtained at temperature $T = 1\epsilon/k_B$ for the stiff polymer of $N = 256$ beads with the bending stiffness $\kappa_b = 22\epsilon$. The time dependence of the potential energy E_p and several conformations drawn from the trajectory at selected points (open circles) are shown. The stages of the polymer collapse include an intermediate state, nucleation, quick tightening, and slow tightening, as indicated.

growth process if the nucleation loop has a large size. Interestingly, these tightening processes dynamically facilitate the formation of the twisted toroidal bundles. It is understood that the twisting requires a polymer to thread through the toroid's hole many times. During the growth process, it is unlikely that the extended part of the polymer can make a threading through the hole. In the tightening processes, the threadings are possible and easier as the polymer ends are located on the toroid and they are pushed through the hole by the same forces that drive the tightening. In principle, a non-twisted toroidal bundle can also convert into a twisted bundle by a structural relaxation without the tightening, but such a relaxation process is much slower and more difficult due to the polymer's topological constraint. Indeed, we find that some trajectories that lack or almost lack a tightening process, like the one shown in Fig. S5, only result in weakly twisted toroidal bundles.

IV. DISCUSSION

The twisted bundle model represents a smooth nematic flow field. Mapping the model to a single chain conformation requires more than a discretization. As described before, the toroidal bundle in this model is organized into disconnected layers of filaments. The bundle in a single layer could be formed by a single filament, such as the one shown in Fig. 1(b), but this may not happen, in general. Connecting the filaments from different layers leads to localized defects.[33] Thus, a single polymer conformation of perfectly uniform twist vector k inside the toroid does not exist. The polymer toroidal bundles obtained in our simulations are far from the perfect one as shown by a strong variation of the local twist vector (Fig. S3). This variation can be due to various factors, such as the small system size, the chain discretization, and the surface effect.

It can be expected that the twisted bundles in the TB-ρ model would lead to a distortion of the hexagonal lattice of filaments as the filament layers in ρ are not twisted in phase. Such a distortion would not be favorable by the intermolecular potentials.[46] Interestingly, our study shows that the TB-ρ model yields only a marginal stability of a few k_BT compared to the TB model. Thus, the uniform twisting should be more favorable if the distortion of the hexagonal lattice in non-uniform twisting comes with a sufficiently high energy cost.

Knotting and unknotting are rare events in polymer dynamics.[47] In a twisted toroidal bundle, as shown in Fig. 1(b), the DNA chain threads through the hole of the toroid many times making the conformation highly knotted. Given $n = \eta(\Delta/d)^2$ is the number of filament crossings found within a toroid tubular cross section, the number of threadings through the hole is roughly equal to $n \cdot k$, with k the twist number. As an estimate, a toroid of 100 nm diameter and a thickness ratio $\alpha = 0.6$ would have about 31 threadings at its optimal twist number. Such a high knotting state would be dynamically inaccessible for a toroid formed by a single chain. However, the situation should be much easier if the toroid is formed by multiple chains. For example, if there are ten chains in the toroid, then each chain would have to make only about three threadings.

DNA is known to have a torsional stiffness associated with elastic responses of the molecule to twist deformations, which correspond to either overwinding or underwinding of the DNA double helix.[48] The torsional stiffness plays an important role in DNA supercoiling, for example in the wrapping of DNA around the histone protein core in nucleosomes.[49] Marko and Siggia[39] showed that the elasticity of DNA also includes a twist–bend coupling arising from the asymmetry between the major and minor grooves of the double helix. Due to this coupling, bending the molecule

induces an unwinding of the helix, whereas overwinding it increases the helix's bending stiffness. There is also a softening of the bending rigidity due to the twist–bend coupling. In Marko and Siggia's model of B-DNA,[39] the twist strain Ω_3 is defined as a deviation of the local twist density from $(\omega_0 - \tau_s)$, where $\omega_0 = 2\pi/l = 1.85\ \text{nm}^{-1}$ is the twist density of DNA in the absence of deformations ($l = 3.4$ nm is the DNA helical pitch) and τ_s is the torsion of the molecular axis [see Eq. (4)]. The torsion in the twisted bundle model can be calculated giving $|\tau_s| < 0.04\ \text{nm}^{-1}$ for toroids of typical sizes. For the DNA conformations with a constant curvature c and a constant torsion τ_s, Marko and Siggia showed that the equilibrium excess twist per helix repeat is $\langle\Omega_3\rangle/\omega_0 = -0.5(D/C)^2(c/\omega_0)^2$[39] for $\tau_s = 0$, where C is the torsional stiffness and D is the twist–bend coupling constant. It was also shown that the case of $\tau_s \neq 0$ leads only to a small correction for $\langle\Omega_3\rangle/\omega_0$ (Fig. 2 of Ref. 39). A recent study has estimated that $C = 110\ \text{nm} \cdot k_BT$ and $D = 40\ \text{nm} \cdot k_BT$.[50] For the DNA in a toroid with the mean radius $R = 40$ nm, using the constant radius of curvature approximation, we get $c = 0.025\ \text{nm}^{-1}$, giving $\langle\Omega_3\rangle \approx -2.2 \times 10^{-5}\ \text{nm}^{-1}$. It comes that the twist energy of the toroid, calculated as $L\frac{1}{2}C\langle\Omega_3\rangle^2$, is less than $0.03k_BT$. Thus, the contribution of the twist energy in toroids is negligible. This result is much different from that for the DNA supercoil on the nucleosome, for which the radius of curvature of DNA is just ~4.5 nm. With such a small radius, the twist–bend coupling can lead to measurable effects.[39,51]

V. CONCLUSION

We have studied several theoretical models for the organization of DNA in toroidal condensates. The results from these models show that the twisted toroidal bundles provide the best stability for toroidal condensates. The two models of twisted bundles considered, one with uniform and the other with non-uniform twisting, yield similar results upon energy minimization. These models show that a moderate twisting can substantially lower the bending energy of the toroid. The degree of twisting of the bundle can be quantified by the twist number k, which determines how quick the change in the rotation angle θ around the toroid tubular axis is compared to the change in the rotation angle ϕ around the toroid main axis along the trace of a DNA filament in toroidal coordinates. The uniformly twisted bundle model shows that the optimal twist number k^*, for the toroid energy is minimized, ranges from 0.66 to 1.12 and depends only on the toroid thickness ratio α.

Interestingly, our REMD simulations show that the ground states of stiff polymers with self-attractive potentials are twisted toroidal bundles, which confirms the finding of the theoretical models. Furthermore, the average twist numbers calculated for the twisted bundles obtained by simulations are close to the optimal twist number k^* predicted by the uniformly twisted bundle model. The constant-temperature simulations of the stiff polymers show that toroids can be formed through a direct pathway or via a hairpin-like or rod-like intermediate with the collapse governed by the nucleation-growth mechanism. The formation of twisted toroidal bundles is dynamically facilitated by the toroid's tightening processes that happen subsequently to the growth process if the toroid formation starts with a large nucleation loop. Due to the topological constraint of the polymer, it is increasingly difficult for a polymer with an increased chain length to access the lowest energy twisted bundle state, as found for the chain of 512 beads. The observation of strongly twisted bundles with sharp U-shaped regions in the simulations suggests that the problem of dynamical accessibility of the twisted bundles can be reduced if the toroid is formed by multiple chains as found in multimolecular DNA condensates.

It has been found that the formations of twisted bundles of filaments and columns are often driven by molecular chirality.[34] The present study, as well as the early one,[33] indicates that toroidal bundles are prone to twisting due to the effect of bending stiffness, in the absence of molecular chirality. It is also shown here that folding of a polymer into the non-trivial structures of twisted toroidal bundles is not as difficult as it seems to be.

SUPPLEMENTARY MATERIAL

See the supplementary material for the curvature maps of the toroids with a thickness ratio $\alpha = 0.9$; for the dependences of the optimal twist number k^*, the mean radius R, and the thickness radius Δ on the surface tension σ of the toroidal condensate in the TB model; for the analysis of the local tangent vectors of the stiff polymers in the toroidal bundles obtained by REMD simulations; for the observation of long-lived metastable states in constant-temperature simulations; for a simulation trajectory showing the formation of a U-shaped region during the toroid growth; and for a simulation trajectory with a conversion from rod to toroid.

ACKNOWLEDGMENTS

Nhung T. T. Nguyen was funded by Vingroup JSC and supported by the Postdoctoral Scholarship Programme of Vingroup Innovation Foundation (VINIF), Institute of Big Data, code VINIF.2021.STS.03. This research was funded by the Vietnam National Foundation for Science and Technology Development (NAFOSTED) under Grant No. 103.01-2019.363.

AUTHOR DECLARATIONS

Conflict of Interest

The authors have no conflicts to disclose.

Author Contributions

Nhung T. T. Nguyen: Data curation (lead); Formal analysis (equal); Funding acquisition (equal); Investigation (lead); Software (supporting); Validation (equal); Visualization (lead); Writing – original draft (equal). **Anh T. Ngo**: Conceptualization (supporting); Formal analysis (supporting); Investigation (supporting); Methodology (supporting). **Trinh X. Hoang**: Conceptualization (lead); Data curation (supporting); Formal analysis (equal); Funding acquisition (lead); Investigation (equal); Methodology (equal); Project administration (lead); Software (lead); Supervision (lead); Validation (equal); Visualization (supporting); Writing – original draft (equal); Writing – review & editing (lead).

DATA AVAILABILITY

The data that support the findings of this study are available from the corresponding author upon reasonable request.

REFERENCES

[1] V. A. Bloomfield, Curr. Opin. Struct. Biol. **6**, 334 (1996).
[2] N. V. Hud and I. D. Vilfan, Annu. Rev. Biophys. Biomol. Struct. **34**, 295 (2005).
[3] L. C. Gosule and J. A. Schellman, Nature **259**, 333 (1976).
[4] H. H. Strey, R. Podgornik, D. C. Rau, and V. A. Parsegian, Curr. Opin. Struct. Biol. **8**, 309 (1998).
[5] T. Maniatis, J. H. Venable, Jr., and L. S. Lerman, J. Mol. Biol. **84**, 37 (1974).
[6] I. D. Vilfan, C. C. Conwell, T. Sarkar, and N. V. Hud, Biochemistry **45**, 8174 (2006).
[7] C. C. Conwell, I. D. Vilfan, and N. V. Hud, Proc. Natl. Acad. Sci. U. S. A. **100**, 9296 (2003).
[8] M. F. V. Pinto, M. C. Morán, M. G. Miguel, B. Lindman, A. S. Jurado, and A. A. C. C. Pais, Biomacromolecules **10**, 1319 (2009).
[9] P. G. Arscott, A.-Z. Li, and V. A. Bloomfield, Biopolymers **30**, 619 (1990).
[10] A. Y. Grosberg and A. V. Zhestkov, J. Biomol. Struct. Dyn. **3**, 859 (1986).
[11] V. V. Vasilevskaya, A. R. Khokhlov, S. Kidoaki, and K. Yoshikawa, Biopolymers **41**, 51 (1997).
[12] H. Noguchi and K. Yoshikawa, J. Chem. Phys. **109**, 5070 (1998).
[13] V. A. Ivanov, M. R. Stukan, V. V. Vasilevskaya, W. Paul, and K. Binder, Macromol. Theory Simul. **9**, 488 (2000).
[14] M. R. Stukan, V. A. Ivanov, A. Y. Grosberg, W. Paul, and K. Binder, J. Chem. Phys. **118**, 3392 (2003).
[15] T. X. Hoang, A. Giacometti, R. Podgornik, N. T. T. Nguyen, J. R. Banavar, and A. Maritan, J. Chem. Phys. **140**, 064902 (2014).
[16] R. Cortini, B. R. Caré, J.-M. Victor, and M. Barbi, J. Chem. Phys. **142**, 105102 (2015).
[17] M. R. Stukan, E. A. An, V. A. Ivanov, and O. I. Vinogradova, Phys. Rev. E **73**, 051804 (2006).
[18] T. X. Hoang, H. L. Trinh, A. Giacometti, R. Podgornik, J. R. Banavar, and A. Maritan, Phys. Rev. E **92**, 060701(R) (2015).
[19] Y. Ishimoto and N. Kikuchi, J. Chem. Phys. **128**, 134906 (2008).
[20] V. V. Vasilevskaya, A. R. Khokhlov, Y. Matsuzawa, and K. Yoshikawa, J. Chem. Phys. **102**, 6595 (1995).
[21] K. Yoshikawa, M. Takahashi, V. V. Vasilevskaya, and A. R. Khokhlov, Phys. Rev. Lett. **76**, 3029 (1996).
[22] T. Sakaue and K. Yoshikawa, J. Chem. Phys. **117**, 6323 (2002).
[23] A. Montesi, M. Pasquali, and F. MacKintosh, Phys. Rev. E **69**, 021916 (2004).
[24] Z. Ou and M. Muthukumar, J. Chem. Phys. **123**, 074905 (2005).
[25] A. Dey and G. Reddy, J. Phys. Chem. B **121**, 9291 (2017).
[26] J. A. Schellman and N. Parthasarathy, J. Mol. Biol. **175**, 313 (1984).
[27] N. V. Hud and K. H. Downing, Proc. Natl. Acad. Sci. U. S. A. **98**, 14925 (2001).
[28] A. Leforestier and F. Livolant, Proc. Natl. Acad. Sci. U. S. A. **106**, 9157 (2009).
[29] K. A. Marx and G. C. Ruben, Nucleic Acids Res. **11**, 1839 (1983).
[30] N. V. Hud, K. H. Downing, and R. Balhorn, Proc. Natl. Acad. Sci. U. S. A. **92**, 3581 (1995).
[31] M. J. Stevens, Biophys. J. **80**, 130 (2001).
[32] J. Arsuaga, M. Vázquez, S. Trigueros, D. W. Sumners, and J. Roca, Proc. Natl. Acad. Sci. U. S. A. **99**, 5373 (2002).
[33] I. Kulić, D. Andrienko, and M. Deserno, Europhys. Lett. **67**, 418 (2004).
[34] G. M. Grason, Rev. Mod. Phys. **87**, 401 (2015).
[35] Y. Sugita and Y. Okamoto, Chem. Phys. Lett. **314**, 141 (1999).
[36] E. Kreyszig, *Differential Geometry* (Dover, New York, 1991).
[37] J. F. Marko and E. D. Siggia, Macromolecules **28**, 8759 (1995).
[38] L. Barberi, F. Livolant, A. Leforestier, and M. Lenz, Nucleic Acids Res. **49**, 3709 (2021).
[39] J. F. Marko and E. D. Siggia, Macromolecules **27**, 981 (1994).
[40] A. Rosa, T. X. Hoang, D. Marenduzzo, and A. Maritan, Macromolecules **36**, 10095 (2003).
[41] B. A. Todd, V. A. Parsegian, A. Shirahata, T. J. Thomas, and D. C. Rau, Biophys. J. **94**, 4775 (2008).
[42] R. H. Swendsen and J.-S. Wang, Phys. Rev. Lett. **57**, 2607 (1986).
[43] P. T. Bui and T. X. Hoang, J. Chem. Phys. **144**, 095102 (2016).
[44] K. Yoshikawa and Y. Matsuzawa, J. Am. Chem. Soc. **118**, 929 (1996).
[45] M. R. Shen, K. H. Downing, R. Balhorn, and N. V. Hud, J. Am. Chem. Soc. **122**, 4833 (2000).
[46] G. M. Grason, Europhys. Lett. **83**, 58003 (2008).
[47] L. Tubiana, A. Rosa, F. Fragiacomo, and C. Micheletti, Macromolecules **46**, 3669 (2013).
[48] P. J. Hagerman, Annu. Rev. Biophys. Biophys. Chem. **17**, 265 (1988).
[49] A. Kaczmarczyk, H. Meng, O. Ordu, J. van Noort, and N. H. Dekker, Nat. Commun. **11**, 126 (2020).
[50] S. K. Nomidis, F. Kriegel, W. Vanderlinden, J. Lipfert, and E. Carlon, Phys. Rev. Lett. **118**, 217801 (2017).
[51] E. Skoruppa, S. K. Nomidis, J. F. Marko, and E. Carlon, Phys. Rev. Lett. **121**, 088101 (2018).